Nonlinear magneto-optic measurement of flux propagation dynamics in thin Permalloy films

T. J. Silva, M. R. Pufall, and Pavel Kabos
National Institute of Standards and Technology, Boulder, Colorado 80305

(Received 7 June 2001; accepted for publication 26 September 2001)

Time-resolved nonlinear optics are used to study the propagation of magnetic flux pulses in a 250 nm Permalloy film. The flux is generated in the film by coupling it to a coplanar waveguide structure driven with broadband voltage pulses. Flux pulses propagated in the film with a phase velocity of 4.2×10^5 m/s and a group velocity of 1.5×10^5 m/s. Both velocities are consistent with the predictions of Damon–Eshbach theory for magnetostatic surface waves with 200–300 μm wavelengths. Within 100 μm of the excitation source, flux pulses decayed monotonically but with no measurable delay. © *2002 American Institute of Physics.* [DOI: 10.1063/1.1421040]

I. INTRODUCTION

Transmission line models for thin-film recording heads are based upon the assumption that flux propagates instantaneously within the head.[1–3] As data rates approach gigahertz bandwidths, the need arises to quantify the validity of such an assumption by measuring the speed of flux propagation in recording head materials. In addition, there is a need to understand the roles of both large magnetization rotations and nonuniform modes possibly excited in the process of such large excitations. To address such issues, it is not sufficient to simply apply a frequency dependence to the permeability, as was done in Ref. 1. Such an improvement to recording head models still fails to account for the time required for flux induced at the yoke to propagate through the poles to the gap. While it is well understood that magnetization response to rf magnetic fields is strongly affected by precessional dynamics (for example, in ferromagnetic resonance), the important question to answer is how magnetic flux propagates in a regime of precession-limited dynamics.

In this article, we experimentally address some aspect of flux propagation dynamics at the surface of a magnetic film by using the second harmonic magneto-optic Kerr effect (SHMOKE) to make time-resolved, vectorial measurements of $\mathbf{M}$.[4,5] The magnetization of the film was driven through near-90° rotations by the pulsed magnetic field from a coplanar waveguide. Quantitative assessments of the phase velocity, group velocity, and attenuation length of a magnetic flux excitation are presented. We show that flux propagation is indeed precession-limited at gigahertz bandwidths. The experimental evidence suggests that oscillatory excitations similar to Damon–Eshbach magnetostatic surface waves are the predominant mechanism of magnetostatic flux transmission, albeit for conditions of large-angle excitation.

II. EXPERIMENT

Waveguide technology has been used effectively for the study of magnetodynamic response to pulsed magnetic fields.[6,7] The coplanar geometry is particularly well suited for studies of planar magnetic films because the transverse field component directly above the waveguide center conductor is relatively uniform on the scale of the waveguide width.[7,8] For the present study it was necessary to clearly distinguish between direct excitations due to the field of the waveguide itself, and those excitations due to the propagation of flux. By minimizing the spacing between the magnetic film and the waveguide, one can obtain a steep roll-off of the transverse field profile at the edge of the center conductor.[7] Consequently, magnetization dynamics measured above the center conductor will be primarily field-induced, while dynamics measured well away from the edge of the center conductor will be primarily due to flux propagation effects. To minimize the sample-waveguide spacing, we placed the sample upside-down on the waveguide and used an optically transparent substrate for the magnetic sample. This permitted placement of the sample in virtual contact with the waveguide conductors, while still allowing optical access through the substrate.

The sample was a 250-nm-thick Permalloy film, sputter deposited directly onto a 1×1 cm$\times100$-μm-thick sapphire substrate, using a single $Ni_{81}Fe_{19}$ alloy target. The film deposition rate was 0.8 nm/s at 300 W and 0.67 Pa (5×10^{-3} Torr) Ar pressure. The base pressure for the deposition chamber was 1.3×10^{-6} Pa (10^{-8} Torr). A 2.8 kA/m (35 Oe) field was applied with permanent magnets during deposition to set the magnetic anisotropy axis. Both the sample and magnets were rotated at one revolution per minute to maintain an isotropic texture to the polycrystalline sample. The sample thickness is the maximum possible before eddy currents begin to severely damp the dynamic response.[9] Sapphire was selected for its transparency at both UV and IR wavelengths and for its excellent thermal conductivity. The thermal conduction of the substrate must be sufficient to permit the focusing of the laser beam with 5 mW of average power to a 5 μm diameter spot without thermally damaging the sample. The small thickness of the substrate minimized unwanted polarization effects induced by the birefringent sapphire. The sample was a well-oriented, high-permeability, polycrystalline Permalloy film, with coercivity H_c of 40 A/m (0.5 Oe), and an anisotropy field H_k of 240 A/m (3 Oe), as measured with an inductive magnetometer. The air surface of the Permalloy film was spin coated with polyamide, with a nominal

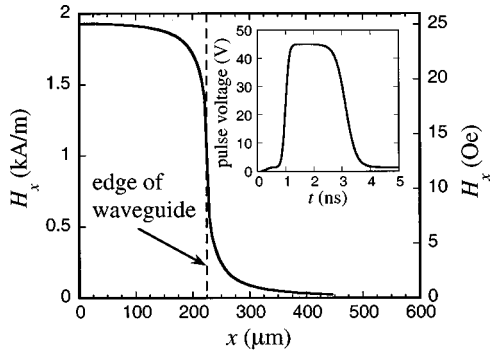

FIG. 1. Profile of transverse magnetic field 1 μm above a 450-μm-wide center conductor for a coplanar waveguide. The contribution of the semi-infinite ground planes to the field is ignored. The waveguide is centered about $x=0$, calculated using the Karlqvist equation with two infinitesimally thin current sheets spaced 23 μm apart. Inset shows time trace of voltage pulse used to generate the magnetic field pulse.

thickness of <1 μm, to avoid electrical shorting of the waveguide by the metallic sample.

The sample was positioned film-side-down over the 450-μm-wide center conductor of a 50-Ω coplanar waveguide. The easy axis was aligned with the waveguide. An 80 A/m (1 Oe) easy axis field was applied during all measurements to ensure single domain behavior. The waveguide itself was made lithographically, patterned from 25-μm-thick Cu on Duroid.[10] The edges of the ground planes on either side of the center conductor are spaced 570 μm from the center of the waveguide in order to achieve 50-Ω characteristic impedance. The waveguide was terminated with a short to double the amplitude of the magnetic field pulse, because the pulse reflected from the short will be superimposed on the incident pulse. All measurements were made within 5 mm of the short to minimize effects resulting from the staggered arrival at the sample of the incident and reflected current pulses.[11] Measurements were also made no less than 2 mm from the edge of the sample to avoid spurious effects due to closure domains. 45 V pulse excitations from a commercial 50-Ω source were applied to the coplanar waveguide to produce a 2 ns long magnetic field pulse with a rise time of 150 ps. An electronic delay line was used to synchronize the arrival of electrical excitation and the optical probe at the sample. The delay line had a measured jitter of 10–20 ps, which limited the measurement bandwidth to 18 GHz. The temporal profile of the voltage step, as measured with a 20 GHz sampling oscilloscope, is shown in Fig. 1. Time-domain reflectometry measurements of the electrical excitations showed that sample-induced reflections due to impedance mismatch were less than 10%. To scan the laser spot laterally across the waveguide/sample, the entire waveguide was mounted on a linear translation stage driven by a dc-servo motor with sub-μm resolution.

The skin depth of copper at 1 GHz is 2 μm. Since the copper sheeting of the waveguide is 25 μm thick, we can assume that most of the current is concentrated within the upper and lower surfaces of the copper sheet. The spatial profile of the transverse magnetic fields is approximated with the Karlqvist equations for two uniform current sheets of infinitesimal thickness, spaced 23 μm apart.[12] The calculated field profile, for an assumed spacing above the upper current sheet of 2 μm, is shown in Fig. 1. We ignore the field contribution from the ground planes for two reasons: (1) Each of the two ground planes is 1 cm wide, resulting in a uniform current distribution that is only 2.5% of that in the center conductor. (2) The fields from the ground planes should only be significant for $x>500$ μm. (For this reason, we only present data for $x<500$ μm.) From such a calculation it is clear that the transverse field falls off rapidly beyond the edge of the center conductor (CC). Thus dynamic data obtained ~ 10 μm beyond the CC edge should represent primarily propagating components of flux. Measured dynamics in this region will result predominantly from the internal dipole fields of the magnetic film.

The dynamic measurements were performed utilizing the vectorial time-resolved SHMOKE technique.[4,5] The 60 fs, *p*-polarized, 800-nm wavelength light pulses were generated by a mode-locked Ti:sapphire laser. The pulse repetition rate was set to 1 MHz using a pulse picker. The laser beam was focused at an angle of 45° through the sapphire substrate to the Permalloy–sapphire interface of the sample. Measurements of the second harmonic generation (SHG) yield versus focal point confirmed that the Permalloy–sapphire interface was the only significant source of SHG for these measurements. Similar measurements were used to keep the spot size greater than 5 μm at the Permalloy–sapphire interface in order to avoid sample degradation due to excessive heating.[13]

SHMOKE is particularly sensitive to surface and interfacial magnetization states as a result of the reduced symmetry required for SHG in centrosymmetric materials.[14,15] As a result, our technique measures the magnetization response within a few nanometers of the Permalloy–sapphire interface. Thus dynamic SHMOKE directly measures the spin dynamics in that portion of the sample where the applied field is not screened by the eddy currents generated as a result of the time-varying magnetization.[16] [The skin depth of a metal with the resistivity of Permalloy is approximately 10 μm. Thus the applied field pulse is able to fully penetrate the magnetic film during the 150 ps rise time of the pulse, but the response of the magnetization (with a rise time of ≈ 1 ns) is inhibited by the much larger eddy currents that result from the rotation of the magnetization.]

The in-plane component of the magnetization vector was determined from the simultaneous measurement of the longitudinal and transverse SHMOKE signals.[5] These signals correspond to the measured polarization angle and total intensity of the SHG, respectively.

Dynamic response of the magnetization in a thin film with in-plane anisotropy generally results in a transient polar magnetization component due to elliptical precission.[17] The ellipticity of the processional motion is $\sqrt{H/M_s}=0.05$. For a 90° rotation of the magnetization, the out-of-plane motion is only 4°. This is sufficiently small to be considered negligible for these measurements.

Flux propagation effects were determined by measuring the dynamic magnetization response at 100 ps time intervals for 6 ns. These time traces were measured at several loca-

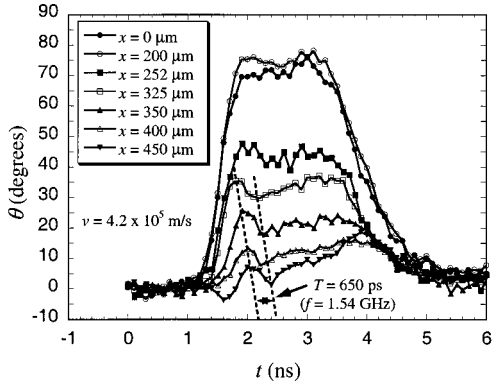

FIG. 2. Time-resolved data measured at different locations relative to the waveguide center. Data for $x>225$ μm are beyond the physical edge of the center conductor. Clear precessional oscillations with a 650 ps period are indicated for $x>300$ μm. The phase of the oscillations is retarded in proportion to x with a measured phase velocity $v=4.2\times10^5$ m/s.

tions relative to the center of the waveguide. A one-dimensional spatial map was thereby constructed, representing the cross-sectional dynamic behavior of **M**, both over the center conductor, and well away from its edge.

III. RESULTS

The measured time response of the magnetization rotation angle is shown in Fig. 2 for several locations on the sample. The middle of the waveguide is at $x=0$ μm, with the edges of the center conductor at $x\sim\pm225$ μm. The collective data set indicates both the generation of magnetic flux pulses and their subsequent propagation over distances of hundreds of micrometers.

The flux pulses for $x<225$ μm (i.e., over the center conductor) closely resemble the applied field pulse profile (see Fig. 1). The field pulse almost saturates the magnetization over the center conductor, inducing a maximum rotation angle of roughly 80° relative to the longitudinal direction. Complete saturation was expected, given a maximum magnetic pulse amplitude of 2 kA/m (25 Oe). In the limit of an infinitely wide sample and small excitations, the effective shape anisotropy due to the finite waveguide width is $H_k\sim\pi M_s\delta/4w=280$ A/m (3.5 Oe), where w is the waveguide width and δ is the film thickness.[18] With the above-listed Permalloy film parameters, as well as the 80 A/m (1 Oe) easy axis stabilizing field, one would expect the applied field pulse to completely saturate the magnetization in the transverse direction directly over the waveguide. Total saturation is achieved when a 50-nm-thick Permalloy film is measured, suggesting that the larger dipole fields produced in the thicker sample are responsible for the incomplete saturation.

Damped oscillations are evident in the flux pulses for all the measured positions. However, the oscillations are strongly damped over the waveguide ($x<225$ μm traces). Fitting of the data at $x=0$ μm to the Landau–Lifshitz–Gilbert equation yields a damping coefficient of $\alpha=0.04$. In contrast, the oscillations (as a relative fraction of the total response) become substantial for $x>325$ μm. Thus precessional dynamics are involved in the propagation of flux away from the waveguide. The period of the oscillations is $T=650\pm50$ ps, corresponding to a precessional frequency of $f=1.54\pm0.12$ GHz (as averaged over all the presented traces). At $x=450$ μm, the precessional oscillations begin with a negative excursion. The half cycle time between the negative dip and the first oscillatory maximum is 400 ps, commensurate with a frequency of 1.3 GHz and within error bars for a single observation of the precessional period.

The position of the first maxima and minima of the magnetization rotation angle (connected by dashed lines in Fig. 2 for different positions) also display retardation in time as a function of increasing distance from the edge of the waveguide center conductor ($x>225$ μm). If we consider the position of this maximum in the magnetization rotation angle as a phase front position, the calculated phase velocity is $v=420\pm34$ km/s.

The flux pulses in Fig. 2 also show substantial changes in shape and amplitude with increasing distance from the waveguide. Quantitative analysis of the measured response in terms of integrated pulse shape will be discussed in the next section.

IV. DISCUSSION

The experimental data in Fig. 2 exhibit many aspects of dynamic flux propagation at the surface of thin magnetic films, including amplitude decay, damping, and propagation delay. The observation of magnetization precession and phase retardation effects beyond the center conductor edge strongly suggest the presence of long wavelength ($\lambda\gg1$ μm) spin wave excitations. A substantial theoretical framework exists for describing the behavior of long wavelength spin waves, but only for oscillations of a symptotically small amplitude about a stable equilibrium, and in the limit of dipole–dipole interactions and negligible damping, i.e., the so-called Damon–Eshbach magnetostatic modes of a thin slab.[19,20] However, since the parameters for the present study (large amplitude and broadband excitations) violate many of the fundamental approximations used for conventional magnetostatic mode theory, there is no firm theoretical background available that is directly applicable to the present experimental data. Nevertheless, comparison of the data with the conventional magnetostatic mode theory provides insight into the fundamental physics behind large-amplitude, high-speed flux propagation.

The curves in Fig. 2 show that both the amplitude and shape of the flux pulses change substantially with increasing distance from the center conductor. Peak amplitude drops while the pulse also distorts, making peak amplitude alone a poor figure of merit for flux attenuation and propagation. Instead, we integrate the net flux that passes a given spot on the sample and normalize the integral by the net flux generated by the field pulse at $x=0$. The result is then weighted by the peak flux amplitude at $x=0$.

$$\langle\Phi(x)\rangle=\mu_0\{M_s\sin[\theta(0,t)]\}_{\max}\frac{\int_0^{6ns}M_s\sin[\theta(x,t)]dt}{\int_0^{6ns}M_s\sin[\theta(0,t)]dt}. \quad (1)$$

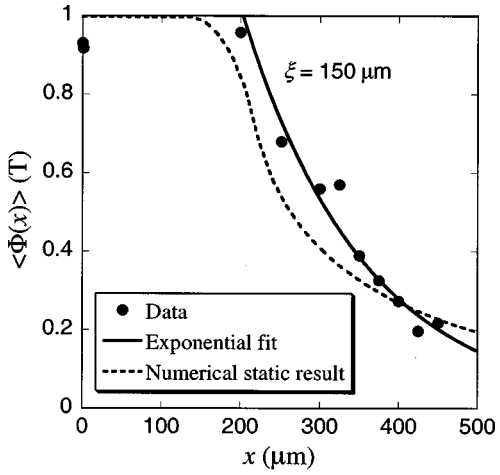

FIG. 3. Weighted integrated flux density vs the distance from the center of the center conductor of the shorted coplanar waveguide. The dashed line is the result of the self-consistent one-dimensional micromagnetic static simulation. The solid line is a simple exponential fit with a characteristics length of 150 μm.

This ''weighted integrated flux'' $\langle\Phi\rangle$ is in units of Telsa and is shown as the solid dots in Fig. 3. The data at $x=0$ μm and $x\approx 220$ μm are roughly the center and the edge of the center conductor of the waveguide, respectively. We can see that the induced flux is quite uniform (to within a few percent), across the center conductor, to within 20 μm of the waveguide edge. Past the waveguide edge, the integrated flux begins to decrease. The solid line is a simple exponential fit to the decaying flux, with a characteristic length of $\xi=150\pm 13$ μm, given 0.05 T error bars. For comparison, the dashed line is the result of a self-consistent, micromagnetic, one-dimensional static calculation of the equilibrium flux distribution, as expected from the field distribution given by the Karlqvist equation in the dc excitation limit. The calculation assumes that **M** varies only in the direction transverse to the waveguide, i.e., **M** is uniform along the length of the waveguide, and also through the thickness of the film.

The micromagnetic simulation does not fit the data well. We surmise that the magnetization distribution has not yet reached equilibrium during an excitation pulse of only 2 ns. The detailed shape of the flux pulses measured for $x>325$ μm support this hypothesis: The magnetization rotation angle does not appear to reach an asymptotic value. In addition, the integrated flux off the edge of the center conductor ($x>225$ μm) is greater than the value expected for static calculations. This implies that there is a transient flow of flux away from the center conductor, with a characteristic length scale of 150 μm.

Some form of precessional excitation, driven by the large magnetization rotations directly over the waveguide, must mediate flux propagation at subnanosecond time scales. Since the internal dipole fields along the x axis are the primary driving force for flux propagation in this experiment, we expect any spin wave excitations to share a similar character to magnetostatic surface waves (MSSWs),[20] insofar as the dispersion for MSSW modes is most strongly affected by the longitudinal dipole field contribution along the propagation direction.

For our experimental geometry, symmetry mandates that the propagation direction for any modes be perpendicular to the waveguide axis. Since the sample of thickness δ and magnetization M_s is placed on the waveguide with the easy axis parallel to the waveguide axis, this constrains the wave vector **k** parallel to the hard axis. The dispersion relation for MSSW modes, in the limit of long wavelength ($k\delta\ll 1$) and weak fields ($H\ll M_s$), is given by[21]

$$\omega(x)\approx\gamma\mu_0\sqrt{[M_s\chi(k)]\{M_s[1-\chi(k)]\sin^2\theta+H_p(x)\cos\theta+H_b\sin\theta-H_k\cos(2\theta)\}}, \tag{2}$$

with

$$\chi(k)=[1-\exp(-k\delta)]/k\delta, \tag{3}$$

where γ is the gyromagnetic ratio, μ_0 is the permeability of free space, θ is the magnetization direction relative to the propagation direction, H_b is the applied bias field parallel to the easy axis, $H_p(x)$ is the pulsed field parallel to the hard axis, and H_k is the uniaxial anisotropy field. The phase velocity v is simply $v=\omega/k$ and the group velocity v_g is given by $v_g=d\omega/dk$.

Because the flux pulse shape is significantly distorted with distance, determining a group velocity must be done with some discretion. A ''center-of-mass'' (C_g) approach has been used successfully in the past to measure the group velocity of magnetostatic waves in nonlinear dispersive media.[22] The C_g for a given pulse is calculated by integrating the measured temporal pulse, with each point weighted by the time variable:

$$C_g=\left[\int_0^{6ns} t\sin[\theta(t)]dt\right]\Big/\left[\int_0^{6ns}\sin[\theta(t)]dt\right]. \tag{4}$$

The derived C_g for the flux propagation data in Fig. 2 are shown in Fig. 4. We define the flux propagation delay as the difference between C_g for a flux pulse at a given position and C_g for the flux pulse in the middle of the center conductor. The flux propagation delay is nominally zero over the center conductor of the waveguide, and remains so up to $x=300$ μm, at which point the propagation delay abruptly begins to increase linearly with increasing distance from the center conductor. The slope of the curve in Fig. 4 is simply the inverse of the group velocity of flux propagation v_g. We performed a linear fit to C_g for $x>300$ μm, and obtained a group velocity $v_g=1.5\pm 0.1\times 10^5$ m/s, with a chi-squared of $\chi^2=1.1$.[23]

We can now compare our measured values for flux propagation time with the theoretical values for MSSW ex-

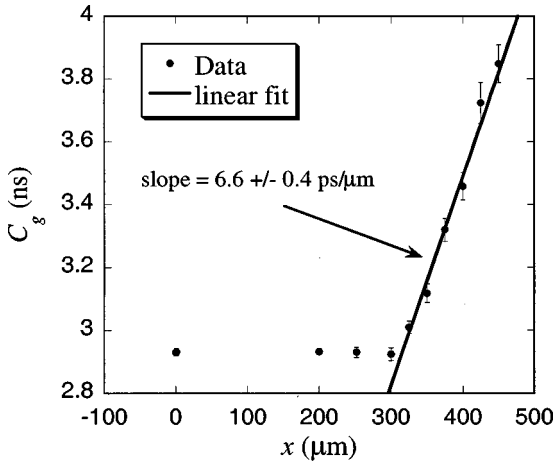

FIG. 4. Flux pulse center-of-mass C_g referenced to the time axis in Fig. 2. Each data point corresponds to time resolved data obtained at a given location. For $x>300$ μm, retardation in C_g is evident, with a linear dependence of C_g on the location. The derived group velocity is $v_g=150$ km/s.

citations. Figure 5 shows the calculated dispersion of the phase velocity for MSSW modes in the long wavelength limit $\lambda \gg \delta$, where δ is the film thickness. Using the measured precessional frequency of $f=1.54\pm0.12$ GHz, one expects from Fig. 5 for the phase velocity to be $v=460\pm50$ km/s, in agreement with the experimental value. The large disparity between the measured group and phase velocities explains the observed negative oscillation at the leading edge of the flux pulse for $x=450$ μm. The phase front is moving three times faster than the energy contained in the pulse. In the time it takes for the phase to advance a full cycle (650 ps), the flux pulse only moves by a third of a cycle (220 ps). The resultant slip between the phase and energy fronts exceeds a half cycle, permitting the phase front to initially undergo a negative excursion.

The mode dispersion directly over the waveguide is strongly affected by both the magnitude of the field pulse and the magnetization rotation. Using Eqs. (2) and (3) we plot the calculated dispersion curves in Fig. 6 for the conditions directly over the waveguide center ($x=0$) during the field pulse, and away from the center conductor ($x>300$ μm), where the field pulse is negligible. The dynamic coupling between these two regions should be maximum for modes that satisfy both energy and momentum conservation. The

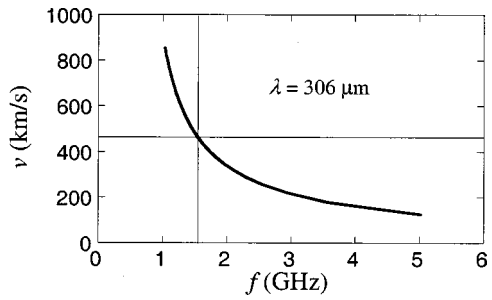

FIG. 5. Calculated phase velocity of the DE surface magnetostatic mode for a 250-nm Permalloy film. The measured phase velocity and precessional frequency for $x>300$ μm are consistent with a 306-μm-wavelength DE surface mode.

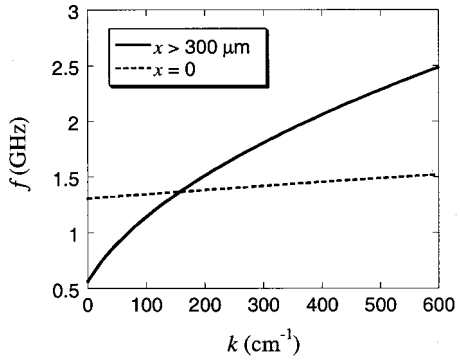

FIG. 6. Calculated dispersion curves for MSSW modes both directly over the waveguide center ($x=0$) and far enough from the center conductor that the field pulse is negligible ($x>300$ μm). The two curves intersect at $f=1.37$ GHz. Modes at this frequency are most likely to escape from the region over the waveguide center conductor.

two curves intersect at $f=1.37\pm0.01$ GHz. (Uncertainty in the measured angle of magnetization rotation in the middle of the waveguide is the primary source of error in our theoretical calculation.) At this frequency, the modes generated over the waveguide conductor are most likely to be coupled to the rest of the film. The measured precession frequency for $x>300$ μm is 40 MHz above the error bars for the theoretical value of the coupling frequency, leaving us with only a qualitative agreement between conventional MSSW theory and our results. This is to be expected, given the gross differences between this experiment and the conditions appropriate for a rigorous application of Damon–Eshbach theory.

The calculated frequency dependence of the MSSW group velocity is shown in Fig. 7. From the earlier-obtained value of $v_g=150$ km/s, we would expect a characteristic frequency of 2.1 GHz. This is well above the measured precession frequency for $x>300$ μm. However, for the present experiments with a 150 ps rise time, the excitation has a characteristic bandwidth of 2.3 GHz. Thus it is possible that the bandwidth of the entire flux pulse is proportional to the bandwidth of the excitation itself. This hypothesis requires further testing before any further conclusions can be made.

The resemblance of the measured flux pulses to MSSW modes is also consistent with the dramatic changes in the

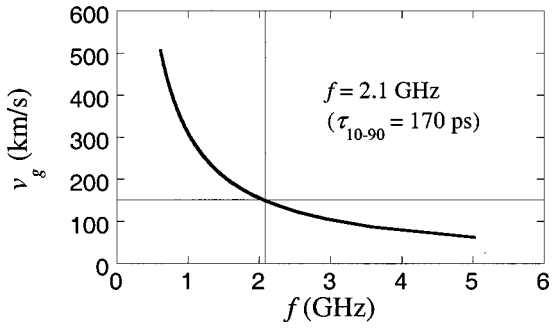

FIG. 7. Calculated group velocity of the DE surface magnetostatic mode for a 250-nm NiFe film. For a measured group velocity of 150 km/s, the characteristic frequency is ~2 GHz. This is within the bandwidth of an excitation pulse with a 150 ps rise time.

measured flux profile: Damon–Eshbach magnetostatic surface waves are highly dispersive,[20] resulting in a strong spatial dependence of the propagating pulse shape.

Fitting of the integrated flux pulse amplitude data in Fig. 3 resulted in a characteristic decay length of $\xi = 150 \pm 13$ μm. The observation of a measurable group delay with increasing separation from the center conductor, together with the poor fit of the data to micromagnetic simulation results for the equilibrium magnetization distribution, suggest that the observed spatial decay is the result of purely dynamic effects, i.e., damping. We can estimate the intrinsic damping time of the flux pulses as $\xi / v_g = 1.1$ ns. This corresponds to a LLG damping parameter of $\alpha = 0.01$, in close agreement to what was measured for 250-nm-thick Permalloy by microwave resonance linewidth techniques ($\alpha = 0.009$).[24]

A comparison of the data in Figs. 3 and 4 indicate differing spatial positions for the onset of flux pulse decay and flux pulse delay. By extrapolation from the linear regression in Fig. 4 we determine an onset of flux pulse delay at $x_0^{\text{delay}} = 317 \pm 37$ μm. The onset of flux pulse decay is determined by the exponential fitting shown in Fig. 3, with the result $x_0^{\text{decay}} = 194 \pm 36$ μm. This is within error bars of the edge of the waveguide center conductor at $x = 225$ μm. In contrast, there is no measurable flux pulse delay unit the flux pulses are located 125 μm beyond the center conductor edge. It appears that the flux pulses have a significant evanescent component within 125 μm of the center conductor edge.

When a magnetic film is driven by a step excitation, frequency components are generated in the film that are below cutoff for MSSW modes. The cutoff for MSSW modes is the ferromagnetic resonance (FMR) frequency for a uniform excitation (i.e., $k = 0$),[25] or 560 MHz for this particular sample. The spectral distribution for a square field pulse with infinitely fast rise and fall time is given by

$$\tilde{H}(\omega) = H_0 T_p \sin(\omega T_p/2)/(\omega T_p/2), \tag{5}$$

where T_p and H_0 are the duration and amplitude of the pulse, respectively. From numerical integration of Eq. (5), 90% of the pulse energy is between dc and 500 MHz, well below the cutoff for MSSW modes. Nevertheless, the low frequency components of the pulse still couple to the magnetic film, as is required to switch the magnetization into the rotated state. However, energy transmission can only occur via evanescent modes at frequencies below cutoff. Such modes, if they exist, should decay monotonically with distance from the excitation source, as we observe in Fig. 3. In addition, such modes would appear to have a very rapid group velocity, since the magnetic energy is transmitted via unidirectional dipolar fields extending throughout the evanescent zone.

Evanescent MSSW modes were first observed using Brillouin light scattering (BLS) for insulator films excited at a single frequency (cw) with a microstrip waveguide.[25] In the BLS study, the evanescent modes were inferred from the detection of MSSW modes at a frequency below cutoff. However, our result differs fundamentally from the BLS study, insofar as the excitation with a stepped field pulse must couple to the magnetization through a process mediated by the relaxation of **M** into the direction of the field pulse. In the BLS study, coupling of the magnetic signal was facilitated by the proximity of a ground plane near the sample, which altered the mode structure.

The absence of any measurable delay due to flux propagation effects within 100 μm of the edge of the waveguide has favorable implications for magnetic recording. The gap of a thin-film recording head is less than 10 μm away from the coils that excite the head. We measured a magnetization rotation angle of 45° at $x = 252$ μm. This position is 27 μm from the waveguide edge. The 10%–90% rise time t_{10-90} of the rotation angle was ~400 ps, with no measurable dispersion due to the flux propagation effects. In other words, the rise time is essentially unchanged relative to that measured over the middle of the waveguide. Given the underdamped response of the magnetization, we can approximate the bandwidth $f_{3\text{ dB}}$ using $f_{3\text{ dB}} \approx 0.5/t_{10-90}$. Thus we find that the effective bandwidth of the magnetic excitation was 1.25 GHz, with an accompanying flux density of $\mu_0 M_s \sin(45°) = 0.71$ T. Since there is no delay of the magnetic response due to the distance between the waveguide and the point of measurement at $x = 252$ μm, the strongest contributor to the nonzero rise time is the precessional motion of the magnetization. The precessional frequency can be accurately estimated using the Kittel equation for ferromagnetic resonance,[26] where the net in-plane fields include the dipole fields due to the excitation of Damon–Eshbach (DE) modes (in the long wavelength limit):

$$f = \frac{\gamma \mu_0}{2\pi} \sqrt{(M_s + H_k + H_{\text{DE}})(H_k + H_{\text{DE}})}. \tag{6}$$

Using $M_s = 800$ kA/m, $H_k = 400$ A/m, and $H_{\text{DE}} = (\pi/2)(M_s \delta / w) = 1.1$ kA/m, where w is the width of the waveguide, we find $f = 1.23$ GHz. This is in good agreement with the measured bandwidth. Thus only the magnetic moment and internal fields of the pole material should ultimately limit the bandwidth of a thin-film recording head. In addition, models of recording head efficiency can safely assume that the flux propagates instantaneously throughout the flux circuit of the head, eddy current effects notwithstanding.

Fitting of the flux pulses observed over the waveguide center conductor to LLG indicated large apparent damping of $\alpha = 0.04$. This is almost a factor of 5 larger than was inferred from the data in Figs. 3 and 4, as well as typical numbers obtained by resonance methods.[24] The observation of an enhanced precessional overshoot at the leading edge of the flux pulses for $x > 300$ μm indicates that the apparent damping may be significantly larger than the intrinsic damping. One of the possible reasons for the larger than expected value of the fitted damping parameter over the waveguide center conductor could be the transfer of energy via magnetostatic modes, which carry the precessional energy away from the portion of the sample in proximity to the center conductor. Using our measured effective group velocity for the flux pulses, we can estimate the magnitude of damping due to the transport of precessional energy away from the directly excited portion of the sample. The energy U that is stored in the form of the precessional motion of **M** directly over the center conductor, immediately after application of the field pulse, is

$$U=\mu_0 M_s H V, \tag{7}$$

where μ_0 is the permeability of the vacuum, M_s is the saturation moment, H is the in-plane component of the applied field pulse, and V is the directly excited volume of the sample. If the field pulse is sufficiently large to rotate **M** by 90°, then the magnon density is[27]

$$N_m=\frac{M_s}{2\gamma\hbar}, \tag{8}$$

where γ is the gyromagnetic ratio and $\hbar$ is Planck's constant. The invocation of spin-wave quanta (i.e., magnons) simplifies the calculation of spin-wave flux. Assuming a spatially uniform distribution of magnons throughout volume V with a single angular frequency ω, then the power P flowing away from the directly excited portion of the sample at group velocity v_g in the form of spin waves propagating through a cross-section $A=2$ V/w is

$$P=N_m\hbar\omega A v_g=\frac{1}{\gamma}M_s\omega A v_g. \tag{9}$$

We will approximate ω with the precessional frequency observed directly over the waveguide, since it is the damping of this component that is directly determined through fitting to LLG. The ratio of Eqs. (7) and (9) is the characteristic time constant $\tau=U/P$ for the excitation decay:

$$\tau=(\gamma\mu_0 H/\omega)(w/v_g), \tag{10}$$

where w is the width of the center conductor of the waveguide. The Gilbert damping parameter α in terms of the decay time τ for a thin film with $M_s \gg H_k$ is

$$\alpha=2/\tau\gamma\mu_0 M_s. \tag{11}$$

Substituting Eq. (10) into Eq. (11), we obtain

$$\alpha=\frac{2\omega}{(\gamma\mu_0)^2 M_s H}\frac{v_g}{w}. \tag{12}$$

Inserting the experimentally observed values for the precession frequency over the center conductor (~1 GHz) and group velocity (150 km/s) into Eq. (12), one gets a value of $\alpha=0.05$, in comparison to the fitted value of $\alpha=0.04$. This is surprisingly good agreement given the crude nature of the above estimate. A more accurate calculation would include a distribution of modes with varying characteristic frequencies, as well as the details of mode coupling between the directly excited portion of the film and those sections extending beyond the waveguide conductor. It should be noted that Freeman *et al.* have suggested a similar damping mechanism to explain time-resolved magneto-optic measurements with YIG films.[28]

V. SUMMARY

We have experimentally measured dynamic flux propagation at the surface of a 250-nm-thick Permalloy film using time-resolved vectorial SHMOKE. The step-like field pulses produced by a shorted coplanar waveguide were nearly sufficient to saturate the sample in the pulse-field direction. The spacing between the sample and waveguide was kept small in order to produce uniform, in-plane excitation fields that rapidly decayed beyond the edge of the waveguide center conductor. Detailed analyses of the data indicate that flux propagation is facilitated by spin waves with qualities suggestive of Damon–Eshbach surface modes. In particular, both the phase and group velocities inferred from the flux pulse data are comparable to those obtained by conventional magnetostatic mode theory.

The measured flux pulse decay was exponential, with a characteristic decay length of 150 μm. The profile of the flux pulse decay did not agree with static micromagnetic calculations, suggesting that flux propagation at GHz bandwidths is truly dynamic in nature and not simply quasistatic.

Flux pulse shapes were severely distorted over propagation distances of several hundred microns, indicating a highly dispersive spin-wave medium. To aid in the extraction of a meaningful flux pulse delay, ''center-of-mass'' analysis methods were employed. The resultant time delays of the centers of mass of the flux pulses were linear in distance from the waveguide, with a slope on the order of 10^5 m/s.

The spatial onset of flux pulse decay and delay are not coincident. Flux pulse decay begins ~100 μm before any measurable flux pulse delay. This discrepancy is interpreted as evidence for an evanescent zone, where the predominant mode of energy transmission is by way of evanescent modes with propagation velocities greater than 10^6 m/s.

Large LLG damping was obtained by fitting of the time-resolved magnetic response over the center conductor. The flux pulse decay length and observation of weakly damped ringing away from the center conductor imply a much smaller intrinsic damping, one which is closer to values typically obtained by FMR. We suggest that flux propagation effects are a significant source of damping near the excitation source. A simple estimate of damping due to spin-wave transport supports this hypothesis.

The implications of these results for magnetic data storage applications are clear: Flux propagation delay should not affect recording head performance as long as yoke and throat lengths are kept much shorter than 100 μm. However, quasistatic calculations of recording head efficiency are certainly invalid at GHz frequencies, since evanescent magnetostatic modes appear to act as the predominant means of energy transmission on these length scales.

[1] E. P. Valstyn and H. Huang, IEEE Trans. Magn. **29**, 3870 (1993).
[2] A. Paton, J. Appl. Phys. **42**, 5868 (1971).
[3] G. F. Hughes, J. Appl. Phys. **54**, 4168 (1983).
[4] T. M. Crawford, T. J. Silva, C. W. Teplin, and C. T. Rogers, Appl. Phys. Lett. **74**, 3386 (1999).
[5] P. Kabos, A. B. Kos, and T. J. Silva, J. Appl. Phys. **87**, 5980 (2000).
[6] M. R. Freeman, M. J. Brady, and J. Smyth, Appl. Phys. Lett. **60**, 2555 (1992).
[7] T. J. Silva, C. S. Lee, T. M. Crawford, and C. T. Rogers, J. Appl. Phys. **85**, 7849 (1999).
[8] T. M. Crawford, T. J. Silva, C. W. Teplin, and C. T. Rogers, Appl. Phys. Lett. **74**, 3386 (1999).
[9] W. P. Jayasekara, J. A. Bain, and M. H. Kryder, IEEE Trans. Magn. **34**, 1438 (1998).
[10] Duroid is a registered trademark of the Rogers Corporation. Certain commercial materials are identified to specify the experimental study adequately. This does not imply endorsement by NIST or that the materials are the best available for the purpose.
[11] T. M. Crawford, P. Kabos, and T. J. Silva, Appl. Phys. Lett. **76**, 2113 (2000).

[12] O. Karlqvist, Trans. R. Inst. Tech. Stockholm **86**, 3 (1954).
[13] T. M. Crawford, C. T. Rogers, T. J. Silva, and Y. K. Kim, Appl. Phys. Lett. **68**, 1573 (1996).
[14] J. Reif, J. C. Zink, C.-M. Schneider, and J. Kirschner, Phys. Rev. Lett. **67**, 2878 (1991).
[15] H. A. Wierenga, W. de Jong, M. W. J. Prins, Th. Rasing, R. Volmer, A. Kirilyuk, H. Schwabe, and J. Kirschner, Phys. Rev. Lett. **74**, 1462 (1995).
[16] R. Wood and M. Williams, IEEE Trans. Magn. **26**, 2954 (1990).
[17] R. J. Hicken and J. Wu, J. Appl. Phys. **85**, 4580 (1999).
[18] A. B. Kos, T. J. Silva, and P. Kabos (unpublished).
[19] M. Sparks, Phys. Rev. B **1**, 3831 (1970).
[20] R. W. Damon and J. R. Eshbach, J. Phys. Chem. Solids **19**, 308 (1961).
[21] K. J. Harte, MIT Lincoln Lab Technical Note 1965-31, 1965 (unpublished).
[22] H. Xia, P. Kabos, R. A. Staudinger, C. E. Patton, and A. N. Slavin, Phys. Rev. B **58**, 2708 (1998).
[23] W. H. Press, B. P. Flannery, W. A. Teukolsky, and W. T. Vetterling, *Numerical Recipes in C* (Cambridge University, New York, 1998), pp. 521–523.
[24] C. E. Patton, J. Appl. Phys. **39**, 3060 (1968).
[25] G. Srinivasan, P. R. Emtage, J. G. Booth, and C. E. Patton, J. Appl. Phys. **63**, 3817 (1988).
[26] C. Kittel, *Introduction to Solid State Physics*, 6th ed. (Wiley, New York, 1986), p. 480.
[27] H. B. Callen, J. Phys. Chem. Solids **4**, 256 (1958).
[28] M. R. Freeman, M. J. Brady, and J. Smyth, Appl. Phys. Lett. **60**, 2555 (1992).